Experimental report

27/08/2021

Proposal: **5-23-739** **Council:** 10/2019

Title: Investigation of the structural influence on the ionic conductivity of iodide argyrodite Li6+xP1-xSnxCh5I

Research area: Materials

This proposal is a new proposal

Main proposer: **Wolfgang ZEIER**

Experimental team: Carolin ROSENBACH
Ananya BANIK
Ajay GAUTAM

Local contacts: Emmanuelle SUARD

Samples: Li6+xP1-xSnxS5I x=0
Li6+xP1-xSnxSe5I x=0.7
Li6+xP1-xSnxSe5I x=0.2
Li6+xP1-xSnxS5I x=0.1
Li6+xP1-xSnxS5I x=0.2
Li6+xP1-xSnxS5I x=0.3
Li6+xP1-xSnxSe5I x=0.3
Li6+xP1-xSnxSe5I x=0.4
Li6+xP1-xSnxSe5I x=0.5
Li6+xP1-xSnxSe5I x=0.6
Li6+xP1-xSnxSe5I x=0.1

Instrument	Requested days	Allocated days	From	To
D2B	2	2	05/09/2020	07/09/2020

Abstract:

The introduction of group IV-element (M = Si/Ge) has been shown to increase the ionic conductivity of Li6P1-xMxS5I by orders of magnitude. However, the Sn-substituted Li6PS5I does not show any significant change in conductivity due to the limited solubility of Sn in the structure. In order to probe the impact of Sn-substitution on the Li-substructure and the associated conductivity, we aim to study the relationship between the structural changes and the ionic conductivity of Li6+xP1-xSnxCh5I (Ch = S, Se) solid solutions. For this, we plan neutron diffraction experiments on Sn- substituted Li6+xP1-xSnxCh5I (Ch = S, Se) solid solutions, which will shed light on the Li-distribution and elucidate the structure-property relationships in this system.

Experimental Report on ILL Proposal 5-23-739

On the Lithium Distribution in Halide Superionic Argyrodites by Halide Incorporation in $Li_{7-x}PS_{6-x}Cl_x$

Superionic lithium argyrodites, Li_6PS_5X (X = Cl, Br, and I) are attractive as electrolytes for all-solid-state-batteries due to their high ionic conductivity originating from structural disorder between the X^-/S^{2-} positions. Replacement of the sulfide by chloride anions (for the series $Li_{7-x}PS_{6-x}Cl_x$) has also shown to increase the conductivity. However, the underlying changes to the lithium substructure were not investigated. Along with the negative x-ray scattering factor of lithium another problem to study these materials via xrd was similar electron density of sulfur and chlorine. Thus, to shed light into the lithium-ion conduction mechanism, here we explore neutron diffraction studies for a large range of nominal halide compositions in this material leading to publication in ACS Appl. Energy Mater (*ACS Appl. Energy Mater*. **2021**, 4, 7, 7309–7315).

$Li_{7-x}PS_{6-x}Cl_x$ samples with x=0.25 steps were synthesized via ball milling of stoichiometric amount of Li_2S, P_2S_5 and LiCl followed by a short annealing step under vacuum as discussed in the published article (*ACS Appl. Energy Mater*. **2021**, 4, 7, 7309–7315). The final argyrodite was hand-ground into powder for neutron diffraction studies. The room temperature neutron powder diffraction data were collected on the D2B high-resolution powder diffractometer at the Institute Laue-Langevin beamline (ILL, Grenoble, France), with monochromatic neutron wavelength $\lambda = 1.594$ Å. Starting point scan was repeated several times at various 2θ values to improve statistics, and each data collection required 4 hours.

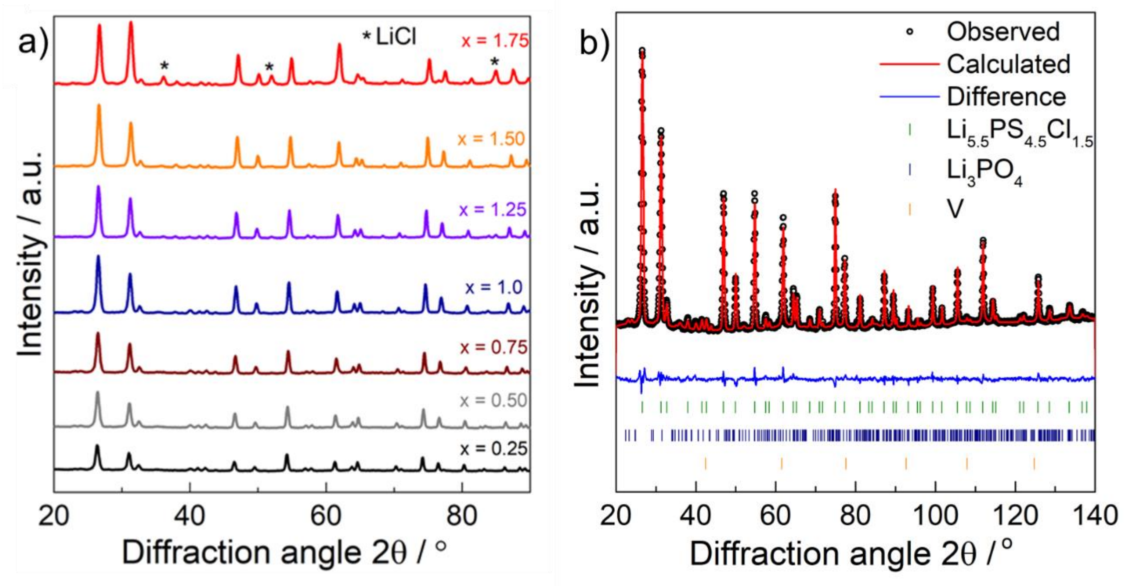

Figure 1: a) Stacked neutron diffraction patterns of the synthesized materials with different chloride content x of for $Li_{7-x}PS_{6-x}Cl_x$. b) Representative Rietveld refinement against neutron diffraction data of $Li_{5.5}PS_{4.5}Cl_{1.5}$. A small fraction of impurity phases corresponding to ~0.7 wt% Li_3PO_4 is present, along with reflections from the vanadium sample container.

Figure 1a shows neutron diffraction patterns for all the samples. To analyse the neutron diffraction data, Rietveld refinements were performed using the TOPAS-Academic V6 software package. All samples exhibited minor impurity phases of Li_3PO_4 (no more than 2.0 wt%). Upon Cl^- substitution from x = 0.25, orthorhombic Li_7PS_6 transforms into cubic crystal polymorph. By further increasing the halide content, lattice parameter decreases indicating enhanced chlorine concentration in the structure; however, the amount of LiCl impurity increases from x = 1.5. Further to understand the influence of increasing Cl^- on S^{2-}/Cl^- disorder, occupancy of S^{2-} and Cl^- on each site were refined (Figure 2a). With rising x, Cl^- prefers to occupy 4*d* site instead of 4*a*. Due to the charge difference of Cl^- and S^{2-}, the average charge on the Wyckoff 4*a* and 4*d* sites will change based on its occupancy. As a direct result of the changing local charge environment, the average surrounding Li^+ substructure is expected to change. Li^+ positions can be directly extracted from the neutron diffraction results. From the refined crystallographic data, the Li^+ distribution is determined. With increasing Cl^- content, the Li^+ "cages" expand, indicated in both decreases of lithium site (T2 – T2) distances and, in a more general sense, increases in the radial distribution of Li^+ away from the center of the cage and hence increases conductivity (Figure 2b).

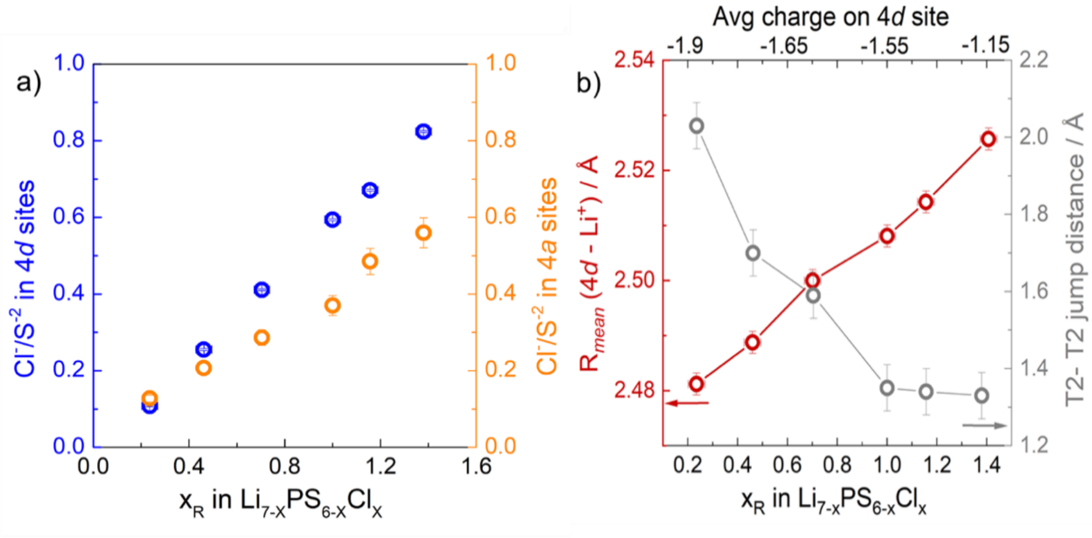

Figure 2: a) The Cl occupancy of the different sites with increasing Cl content in $Li_{7-x}PS_{6-x}Cl_x$. b) R_{mean}, representing the radial distance between the centers of the cage (Wyckoff 4d) and the mean Li density of the surrounding cage, increases, and the T2 –T2 distance (inter-cage jump) significantly decreases with increasing Cl content.

This study explores the understanding of the fundamental structure–transport correlations in the argyrodites, specifically structural changes within the Li^+ ion substructure upon changing anionic charge distribution.